The Application of Computational Fluid Dynamic (CFD) on the Design of High Subsonic Wing

PRASETYO EDI, NUKMAN YUSOFF and AZNIJAR AHMAD YAZID
Department of Engineering Design & Manufacture,
Faculty of Engineering, University of Malaya,
50603 Kuala Lumpur,
MALAYSIA
p_edi@um.edu.my http://design-manufacturer.eng.um.edu.my/

Abstract: - This paper intends to present the application of Computational Fluid Dynamic (CFD) on the design of high subsonic wing of transport aircraft. The computation was performed using RAMPANT, an unstructured, multigrid flow solver. A 2-D and 3-D model of the wing was created using CATIA (2D and 3D modeling). A corresponding grid was created using preBFC and TGrid. The paper describes the technique of creating the grid and using the CFD on the wing design process. It then discusses the benefits and penalties of using the above tools. Description is then given in using the aerodynamic analysis result to optimize the wing. It concludes with a discussion of the results and recommendations for future work.

Key-Words: - computational fluid dynamic (CFD), wing design, aircraft design, aerodynamic configuration

1 Introduction

Many aircraft operate at transonic speed, where part of the flowfield is subsonic and part is supersonic. At these speeds shock waves form on the wings, which cause an increase in drag and variable changes in lift. Multiple shock waves can develop and interact in ways that are difficult to predict, but that have large influences on lift and drag.

With detailed knowledge of the flowfield and shock wave locations, designers can shape the wing to delay the transonic drag rise and increase the lift to drag ratio. These result in higher transonic cruising speeds and reduced fuel consumption.

This flowfield knowledge can be obtained by predicting the chordwise pressure and spanwise distributions and modifying them by geometry changes. The flow around the wing can thus be controlled.

2 Computational Aerodynamics

Computational fluid dynamics is the analysis of systems involving fluid flow, heat transfer and associated phenomena such as chemical reactions by means of computer-based simulation [1]. The use of CFD to predict internal and external flows has risen dramatically in the past decade. Computational methods have revolutionized the aircraft design process. Prior to the mid sixties aircraft were designed and built largely without the benefit of computational tools. Design information was mostly provided by the results of analytic theory combined with a fair amount of experimentation. Analytic theories continue to provide invaluable insight into the trends present in the variation of the relevant parameters in a design. However, for detailed design work, these theories often lack the necessary accuracy, especially in the presence of non-linearities (e.g. transonic flow). With the advent of the digital computer and the fast development of the field of numerical analysis [2, 3 &4], a variety of complex calculation methods have become available to the designer. Advancements in computational methods have pervaded aerodynamics.

Computational methods first began to have a significant impact on aerodynamics analysis and design in the period of 1965-75. This decade saw the introduction of panel methods which could solve the linear flow models for arbitrarily complex geometry in both subsonic and supersonic flow. It also saw the appearance of the first satisfactory methods for treating the nonlinear equations of transonic flow, and the development of the hodograph method for the design of shock free supercritical airfoils.

Panel methods are based on the distribution of surface singularities on a given configuration of interest, and have gained wide-spread acceptance throughout the aerospace industry. They have achieved their popularity largely due to the fact that the problems can be easily setup and solutions can be obtained rather quickly on today's desktop computers. The calculation of potential flows around bodies was first realized with the advent of the surface panel methodology originally developed at

the Douglas company. During the years, additional capability was added to these surface panel methods. These additions included the use of higher order, more accurate formulations, the introduction of lifting capability, the solution of unsteady flows, and the coupling with various boundary layer formulations.

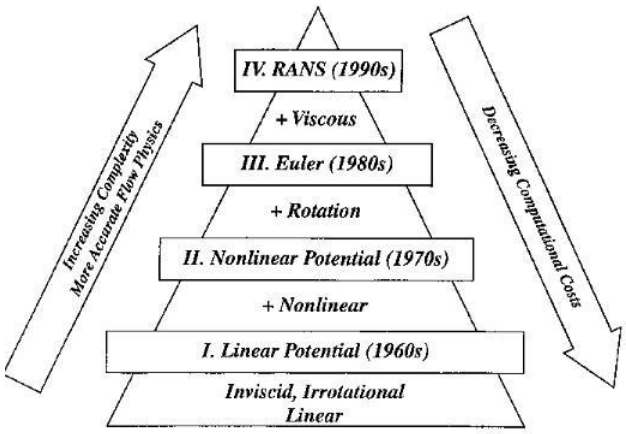

Fig. 1 Hierarchy of aerodynamic models with corresponding complexity and computational cost.

Panel methods lie at the bottom of the complexity pyramid for the solution of aerodynamic problems. They represent a versatile and useful method to obtain a good approximation to a flow field in a very short time. Panel methods, however, cannot offer accurate solutions for a variety of high-speed non-linear flows of interest to the designer. For these kinds of flows, a more sophisticated model of the flow equations is required. Figure 1 indicates a hierarchy of models at different levels of simplification which have proved useful in practice. Efficient flight is generally achieved by the use of smooth and streamlined shapes which avoid flow separation and minimize viscous effects, with the consequence that useful predictions can be made using inviscid models. Inviscid calculations with boundary layer corrections can provide quite accurate predictions of lift and drag when the flow remains attached, but iteration between the inviscid outer solution and the inner boundary layer solution becomes increasingly difficult with the onset of separation. Procedures for solving the full viscous equations are likely to be needed for the simulation of arbitrary complex separated flows, which may occur at high angles of attack or with bluff bodies. In order to treat flows at high Reynolds numbers, one is generally forced to estimate turbulent effects by Reynolds averaging of the fluctuating components. This requires the introduction of a turbulence model. As the available computing power increases one may also aspire to large eddy simulation (LES) in which the larger scale eddies are directly calculated, while the influence of turbulence at scales smaller than the mesh interval is represented by a subgrid scale model.

The codes that are now on the market may be extremely powerful, but their operation still requires a high level of skill and understanding from the operator to obtain meaningful results in complex situations.

2.1 Role of Computational Methods

The role of computational methods in the aircraft design process is to provide detailed information to facilitate the decisions in the design process at the lowest possible cost and with adequate turnaround (turnaround is the required processing time from the point a piece of information is requested until it is finally available to the designer in a form that allows it to be used). In summary, computational methods ought to :

- Allow the simulation of the behavior complex systems beyond the reach of analytic theory.
- Substantial reduction of lead times and cost of new designs, hence increase competitiveness.
- Practically unlimited level of detail of results.
- Ability to study systems where controlled experiments are difficult or impossible to perform (e.g. very large systems).
- Ability to study systems under hazardous conditions at and beyond their normal performance limits (e.g. safety studies and accident scenarios).
- Enhance the understanding of engineering systems by expanding the ability to predict their behavior.
- Provide the ability to perform multidisciplinary design optimization.

Computational methods are nothing but tools in the aircraft designer's toolbox that allow him/her to complete a job. In fact, the aircraft designer is often more interested in the interactions between the disciplines that the methods apply to (aerodynamics, structures, control, propulsion, mission profile) than in the individual methods themselves. This view of the design process is often called multidisciplinary design (one could also term it *multidisciplinary computational design*). Moreover, a designer often wants to find a combination of design choices for all the involved disciplines that produces an overall better airplane. If the computational prediction methods for all disciplines are available to the designer, optimization procedures can be coupled to

produce *multidisciplinary design optimization* (MDO) tools.

The current status of computational methods is such that the use of a certain set of tools has become routine practice at all major aerospace corporations (this includes simple aerodynamic models). However, a vast amount of work remains to be done in order to make more refined non-linear techniques reach the same routine use status. Moreover, MDO work has been performed using some of the simpler models, but only a few attempts have been made to couple high-fidelity non-linear disciplines to produce optimum designs.

2.2 Potential Problems Arising from the Misguided Use of Computational Techniques

Although computational methods are a wonderful resource to facilitate the process of aircraft design, their misuse can have catastrophic consequences. The following considerations must be always in the aircraft designer mind when him/her decide to accept as valid the results of a computational procedure :

- *A solution is only as good as the model that is being solved* : if the aircraft designer try to solve a problem with high non-linear content using a computational method designed for linear problems, the results will make no sense.
- *The accuracy of a numerical solution depends heavily on the sophistication of the discretization procedure employed and the size of the mesh used*. Lower order methods with underresolved meshes provide solutions where the margin of error is quite large.
- *The range of validity of the results of a given calculation depends on the model that is at the heart of the procedure*: if the aircraft designer are using an inviscid solution procedure to approximate the behavior of attached flow, but the actual flow is separated, the results will make no sense.
- *Information overload*. Computational procedures flood the designer with a wealth of information that sometimes is complete nonsense! When analyzing the results provided by a computational method do not concentrate on how beautiful the color pictures are, be sure to apply the knowledge of basic principles, and make sure that the computational results follow the expected trends.

2.3 Computational Cost

The variable cost of an experiment, in terms of facility hire and/or man-hour costs, is proportional to the number of data points and the number of configurations tested. In contrast CFD codes can produce extremely large volumes of results at virtually no added expense and it is very cheap to perform parametric studies, for instance to optimise aircraft performance. Computational costs vary drastically with the choice of mathematical model. Panel methods can be effectively used to solve the linear potential flow equation with personal computers (with an Intel 486 microprocessor, for example). Studies of the dependency of the result on mesh refinement have demonstrated that inviscid transonic potential flow or Euler solutions for an airfoil can be accurately calculated on a mesh with 160 cells around the section, and 32 cells normal to the section. Using multigrid techniques 10 to 25 cycles are enough to obtain a converged result. Consequently airfoil calculations can be performed in seconds on a Cray YMP, and can also be performed on 486-class personal computers. Correspondingly accurate three-dimensional inviscid calculations can be performed for a wing on a mesh, say with 192 x 32 x 48 = 294,912 cells, in about 20 minutes on a high-end workstation (SGI R10000), in less than 3 minutes using eight processors, or in 1 or 2 hours on older workstations such as a Hewlett Packard 735 or an IBM 560 model.

Viscous simulations at high Reynolds numbers require vastly greater resources. Careful studies have shown that between 20 and 32 cells in the normal direction to the wall are required for accurate resolution of the boundary layer. In order to maintain reasonable aspect ratio in all the cells in the mesh (for reasons of numerical accuracy and convergence) on the order of 512 cells are necessary in the direction wrapping around the wing, and at least 64 cells are required in the spanwise direction. This leads to over 2 million cells for a minimally resolved viscous wing calculation. Reynolds Averaged Navier-Stokes calculations of this kind can be computed in about 1 hour on a Cray C-90 computer or over 10 hours in a typical high-end workstation. These computations not only require powerful processors; they also need computers with large memory sizes (1-2 Gb for this kind of calculations). The computer simulations save US$ 150,000 during the development of the new commuter jet by reducing the need for some wind tunnel testing and flight tests [5].

2.4 The Organizational Structure of Computation

CFD codes are structured around the numerical algorithms that can tackle fluid flow problems. In order to provide easy access to their solving power all commercial CFD packages include sophisticated user interfaces to input problem parameters and to examine the results. Hence all codes contain three main elements : (i) a pre-processor, (ii) a solver and (iii) a post-processor. The aerodynamic computation uses in this work consists of :

- **CATIA**, pre-processor for 2D and 3D geometry modeling. For 3D complex geometry modeling, CATIA has better capability than preBFC.
- **preBFC**, pre-processor for 2D and 3D simple geometry modeling, unstructured 2D-mesh generator, and unstructured surface mesh generator.
- **TGrid**, pre-processor for 3D-volume mesh : 2D (triangular) and 3D (tetrahedral) mesh generator.
- **RAMPANT**, the solver and post-processor.

Figure 2 shows aerodynamic calculations program structure uses in this work.

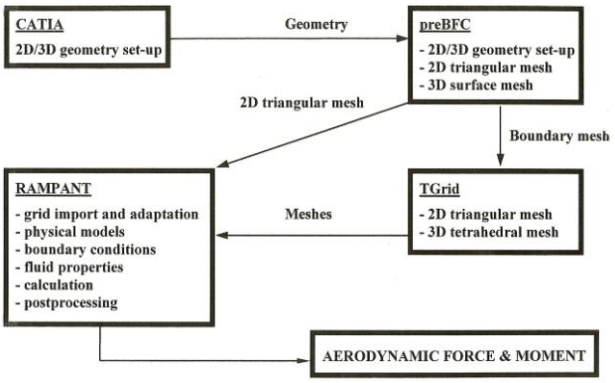

Fig. 2 Aerodynamic calculations program structure

2.5 Computational Verification

A study was made to verify the use of RAMPANT as a primary wing design tool in this work. The verification was made both on two-dimensional and three-dimensional configurations [6].

2.5.1 Two-Dimensional Problem

A laminar flow airfoil, NLF-5 [7], was selected for this study. This airfoil has a thickness to chord ratio of 10.1 %, a design section lift coefficient of 0.5, and is intended to cruise at M = 0.78.

The comparison of pressure distribution of the NLF-5 airfoil between Boeing and RAMPANT is shown in Figure 3. The results shown here are for M_∞ = 0.78, angle of attack = 0 degree, and Reynolds number of 20.6×10^6. The computational domain is rectangular box that extends 25 chord lengths in front, behind, above, and below the airfoil. The NLF-5 airfoil mesh contains 6,218 nodes, 17,627 faces and 11,409 cells. Inviscid flow was assumed for the computations.

The pressure distribution predicted by RAMPANT is in fair agreement with the calculated data from Boeing. The shock position and strength are quite close. According to the RAMPANT predictions, the NLF-5 airfoil has more lift aft of the shock and less lift in the front of shock, hence more pitching moment.

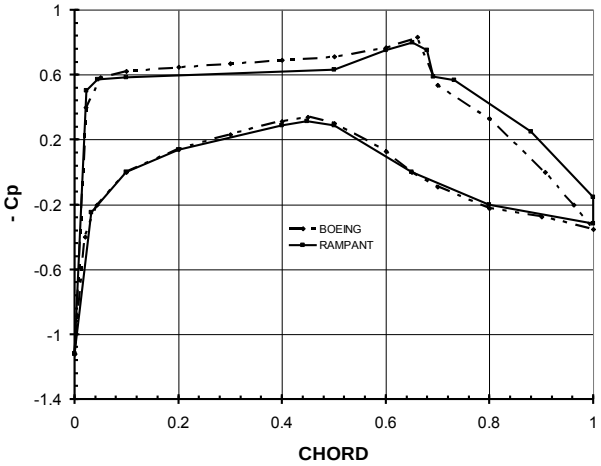

Fig. 3 Pressure distribution of NLF-5 Airfoil

2.5.2 Three-Dimensional Problem

The NACA 0012 wing, based on NASA [8], was selected for this study. The wing has an aspect ratio of eight and a NACA 0012 airfoil, without twist. The planform has a taper ratio of 0.5 and a leading-edge sweep angle of 20 degrees. The wing is attached to a cylindrical fuselage (no fuselage geometry data are given).

The comparison of pressure distributions at spanwise stations (2y/b) = 0.46 of the NACA 0012 wing between NASA and RAMPANT is shown in Figure 4. The results shown here are for M_∞ = 0.85, angle of attack = 2 degrees, and Reynolds number based on the mean aerodynamic chord of 9×10^6. The computational domain is a rectangular box that extends 8.3 fuselage lengths in front, behind, above, and below the wing, and 7.8 wing semispans to the side of the wing. The domain mesh contains 55,593 nodes, 556,852 faces, and 267,874 cells. Inviscid flow was assumed for the computations.

The pressure distribution predicted by RAMPANT at spanwise station 0.46 is in fair agreement with the calculated data by TIBLT (Transonic Interactive Boundary-Layer Theory) code. A shock is present on the upper surface of the

wing. The shock position predicted by RAMPANT is about 5 % of the chord length aft of the TIBLT prediction. This may be because the grid is not fine enough (because the limitations of available computer memory) to capture the shock.

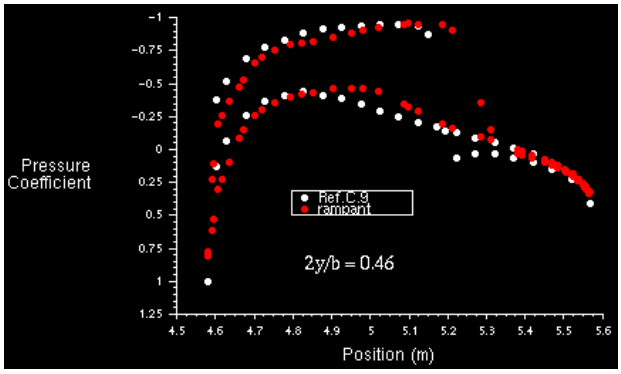

Fig. 4 NACA 0012 wing pressure distributions (Ref.C.9 = Reference 5)

2.5.3 Grid Density Comparison

The following information on the grid density for similar studies can be used as comparisons with the above analysis. Simulations for NLR7301 airfoil were performed for the measurements obtained at the corrected experimental flow conditions of free-stream Mach number of 0.753 and Reynolds number of 1.727×10^6 at an angle of attack of -0.8 degrees [9]. The computational grids are C-type 257x41 and 257x91 points grids respectively for inviscid and viscous computations respectively. The grids have minimum normal spacing at the airfoil surface of 1×10^{-3} and 1×10^{-6} chords respectively for inviscid and viscous computations, with 41 grid points in the wake and with far field boundary extended by 25 chord lengths from the airfoil surface.

Numerical investigations for a wing with high lift devices (slat and flap) were performed at Mach number of 0.22 and a chord-based Reynolds number of 3.7×10^6 at an angle of attack of 10 degrees [10]. The simulation was using 10 chords upstream and 10 chords downstream. Structured, overset grids are used throughout this study. The flap zone used 185x40x75 points, the slat zone used 121x53x27 points. The flapped main element grid used 237x40x81 nodes; the unflapped element grid used 187x56x115 nodes. A slat box for tip vortex identification used a box of 63x85x100 points. The composite mesh contains a total of 3.94 million points within 8 zones. Mesh sizes for the two-element case and the full-span slat case are 2.31 million points and 3.02 million points, respectively.

3 Aerodynamic Wing Design

The main objective of this section was to analyse whether the wing used in this work fulfils the design objectives or not.

The transonic flow over the wing of a typical regional aircraft (W-ATRA) was calculated [6].

3.1 Aerodynamic Design Objectives

The main objectives of the wing design, which incorporates laminar technology are :

a. To obtain a pattern of approximately straight isobar sweep at an angle at least equal to the wing sweepback angle, with the upper surface generally being critical for drag divergence. If this aim is achieved, the flow will be approximately two-dimensional and the drag-divergence will occur at the same Mach number every where along the span.
b. To obtain the greatest possible amount of laminar flow on the wing this will significantly improve wing efficiency (L/D) in cruise flight. The maximum reduction in drag for the wing must be obtained for the cruise C_L corresponding to the design case for the proposed aircraft. To achieve the laminar flow objectives for the design, it was required that the laminar airfoil pressure distributions (suitably interpolated over the span) should be realized by the 3D wing.
c. To have a good performance in off-design operations.

3.2 Configuration Description

For this study, a wing of a typical regional aircraft (W-ATRA) was sized [6] as shown in Figure 5.

To simplify the problem and also to keep the grid size low as possible, the analysis was performed for a half wing-body configuration only. Two flap of baseline configuration were used in this analysis :

a. Configuration I : flap undeployed
b. Configuration II : flap deployed

The variation of VC (variable camber) flap deflection (dvcw) along the span is not optimized yet, but these analyses show the effect of VC-flap deflection on the section pressure distribution along the span.

The wing surface grid of configurations I and II used for this analysis were created. The grids are for $M_\infty = 0.8$, angle of attack = 0 degree, and Reynolds number of 21.6×10^6. The computational domain was a rectangular box that extends a 5 fuselage length in front, behind, above, and below the wing, and 3 fuselage lengths (6.8 wing semispan) to the side of

the wing. The size of the mesh of the above two configurations were as follows :

a. Configuration I = 35,019 Nodes, 344,787 Faces, 165,256 Cells
b. Configuration II = 36,215 Nodes, 355,903 Faces, 170,522 Cells

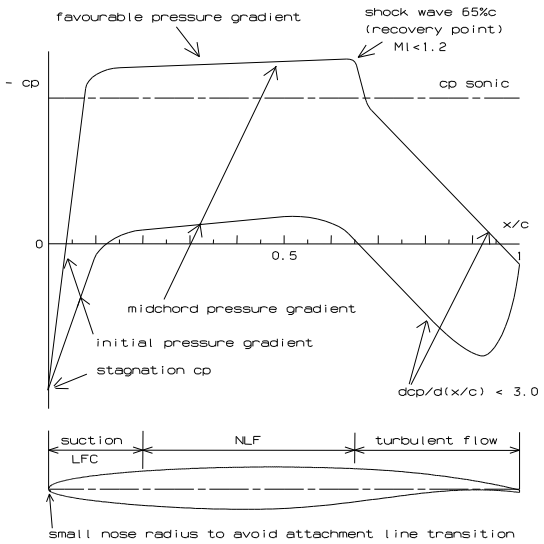

Fig. 5a Airfoil design criteria

Fig. 5b The profile of the root wing aerofoil section

Fig. 5c The profile of the inboard wing aerofoil section

Fig. 5d The profile of the outboard wing aerofoil section

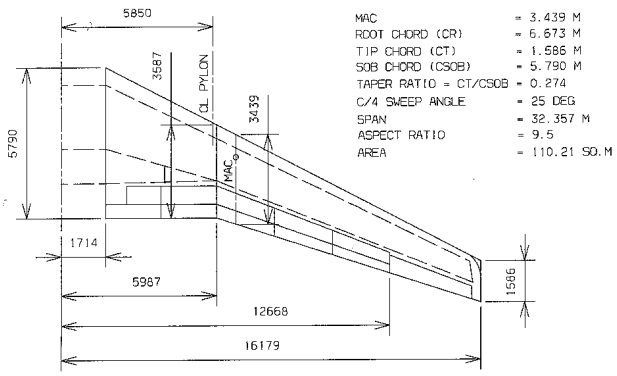

Fig. 5e Wing configuration

3.3 Results

The wing surface pressure and Mach number distributions were measured at 6 different spanwise stations : 2y/b = 0.106, 0.191, 0.37, 0.578, 0.786 and 1.00. Figures 6 and 7 show pressure and Mach number contours on the surface of configuration I. Figures 8 and 9 show pressure and Mach number contours on the surface of configuration II.

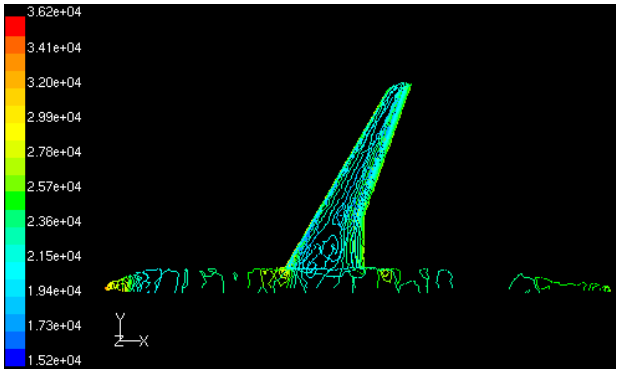

Fig. 6 Configuration I : contours of static pressure

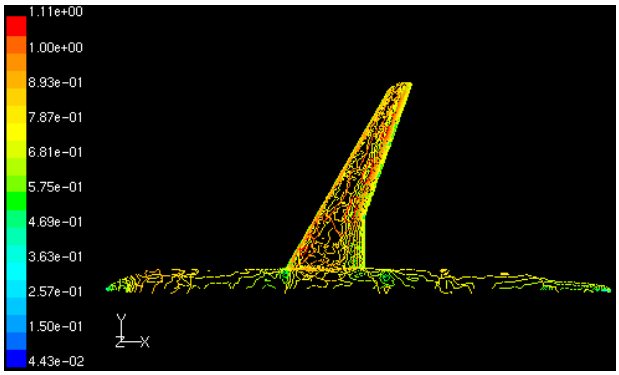

Fig. 7 Configuration I : contours of Mach number

From Figures 6 and 8, for both configurations, the average wing upper surface isobar sweep angle (taken at 50% chord) is approximately 21.8 degrees, instead of 25 degrees (wing quarter chord sweep angle). Thus, the isobar sweep efficiency is = 21.8/25 = 0.872. The inboard wing upper surface isobars are characterized by more sweeps forward at the front and less sweepback at the rear, and the shock strength is quite weak.

The pressure distributions at spanwise stations : 2y/b = 0.106, 0.191, 0.37, 0.578, 0.786 and 1.00 of both configuration I and configuration II are shown in Figure 10.

From Figure 10, for both configuration I and II, it can be seen that all of the pressure distributions (especially on the outboard wing, i.e. : from the kink to the tip) are characterized by a steep initial gradient (rapidly falling pressure), followed by a negative pressure gradient (falling/favourable pressure) and a single weak shock wave and finally

a recovery region with a soft aft pressure gradient. The above pressure distribution characteristics make it is possible to apply the laminar concepts on the wing of both configurations I and II.

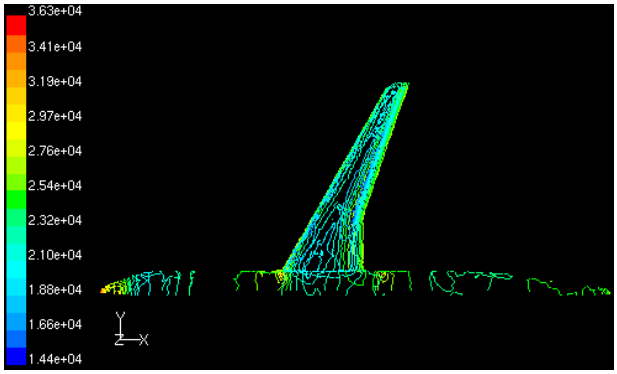

Fig. 8 Configuration II : contours of static pressure

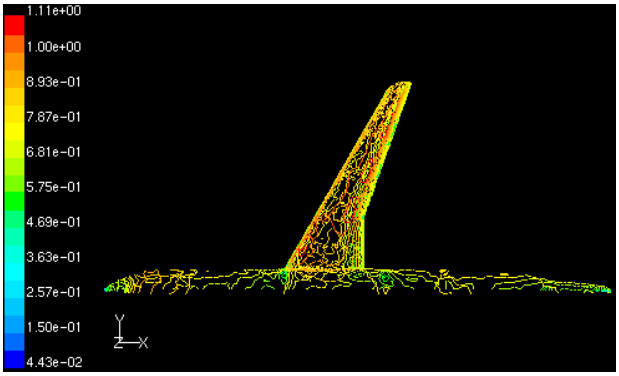

Fig. 9 Configuration II : contours of Mach number

As shown in Figures 10 and 11, with the deflection of VC-flap, the pressure distribution shape at the front of shock does not change too much; this is good for laminar application. The VC-flap deflection makes the shock stronger and increases aft loading (producing greater pitching moment and hence more trim drag).

The spanwise load distribution for configuration I and configuration II are shown in Figure 12. It is very clear the effect of VC-flap deflection on spanwise load distribution, which can be used to optimize it in order to improve the aircraft performances.

At the aircraft design lift coefficient (C_L = 0.5), the comparisons between pressure distribution at subcritical Mach number and design Mach number for the outboard wing sections is shown in Figures 13.

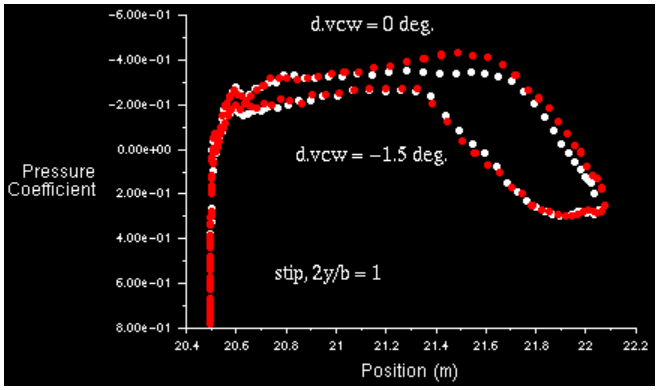

Fig. 10a Configuration I (red) and II (white) at spanwise station (2y/b) = 1.00 : pressure distribution

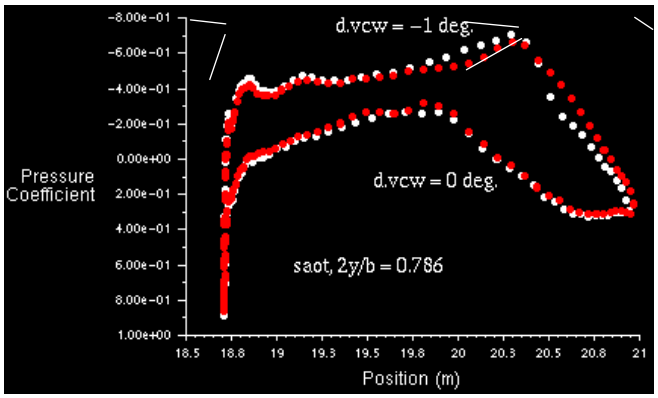

Fig. 10b Configuration I (red) and II (white) at spanwise station (2y/b) = 0.786 : pressure distribution

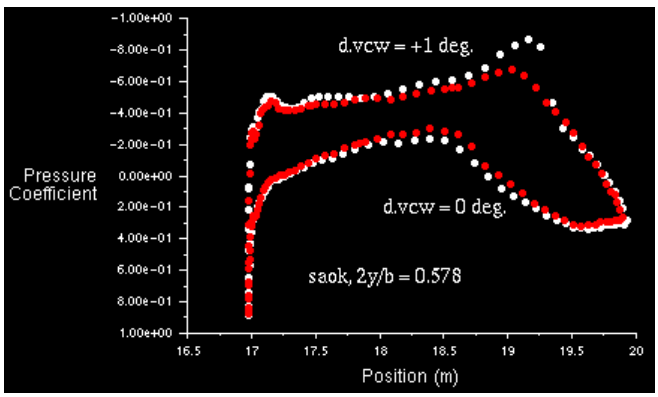

Fig. 10c Configuration I (red) and II (white) at spanwise station (2y/b) = 0.578: pressure distribution

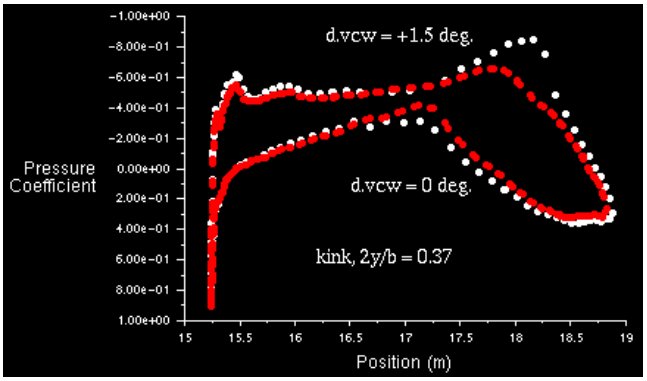

Fig. 10d Configuration I (red) and II (white) at spanwise station (2y/b) = 0.37: pressure distribution

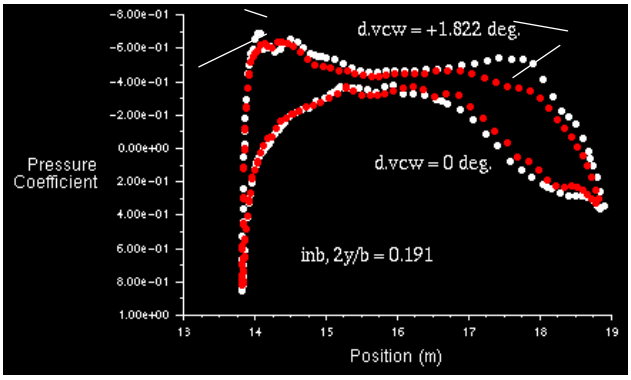

Fig. 10e Configuration I (red) and II (white) at spanwise station (2y/b) = 0.191: pressure distribution

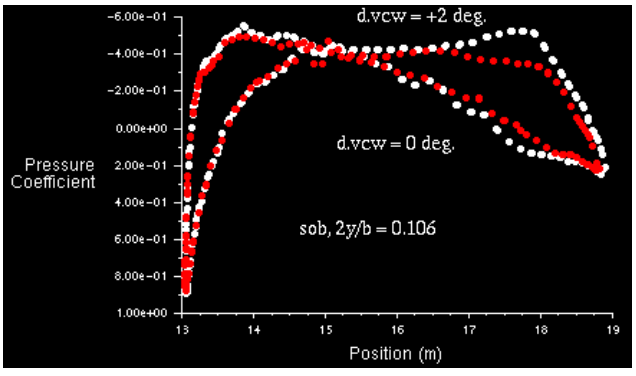

Fig. 10f Configuration I (red) and II (white) at spanwise station (2y/b) = 0.106: pressure distribution

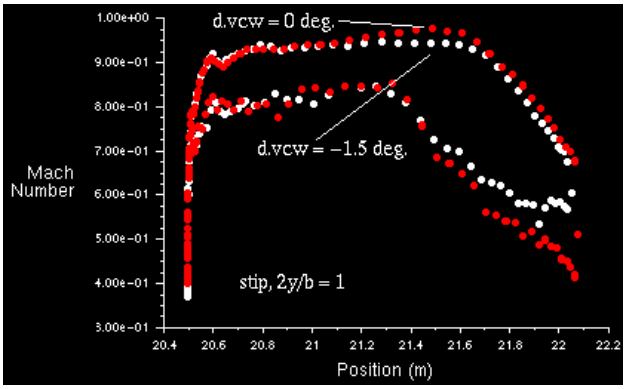

Fig. 11a Configuration I (red) and II (white) at spanwise station (2y/b) = 1.00 : Mach number distribution

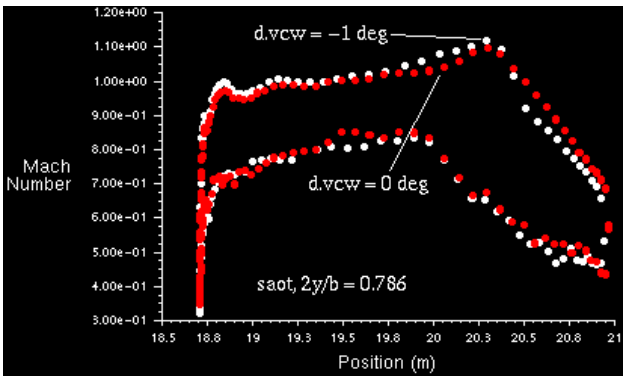

Fig. 11b Configuration I (red) and II (white) at spanwise station (2y/b) = 0.786 : Mach number distribution

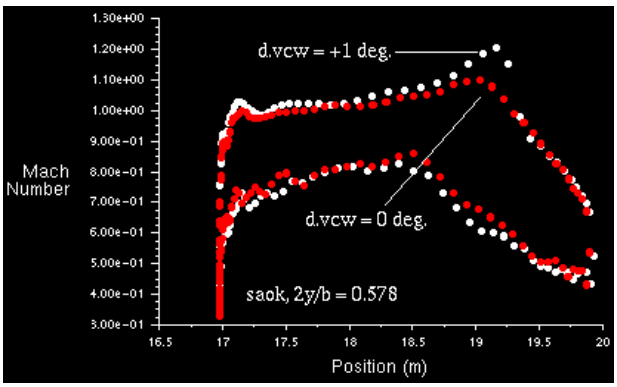

Fig. 11c Configuration I (red) and II (white) at spanwise station (2y/b) = 0.578 : Mach number distribution

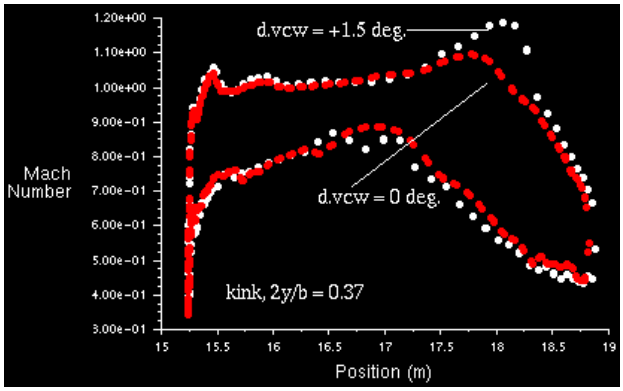

Fig. 11d Configuration I (red) and II (white) at spanwise station (2y/b) = 0.37 : Mach number distribution

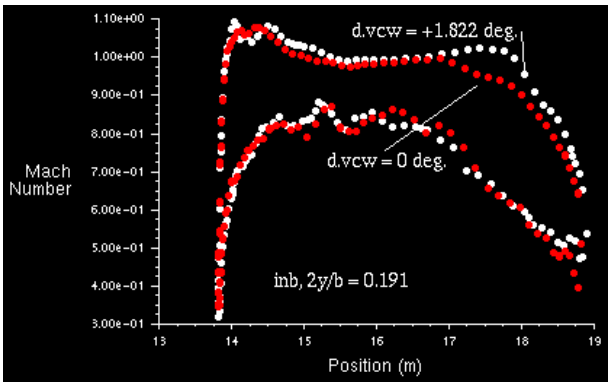

Fig. 11e Configuration I (red) and II (white) at spanwise station (2y/b) = 0.191 : Mach number distribution

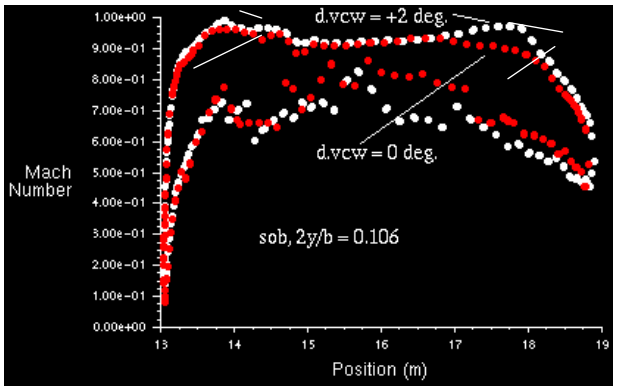

Fig. 11f Configuration I (red) and II (white) at spanwise station (2y/b) = 0.106 : Mach number distribution

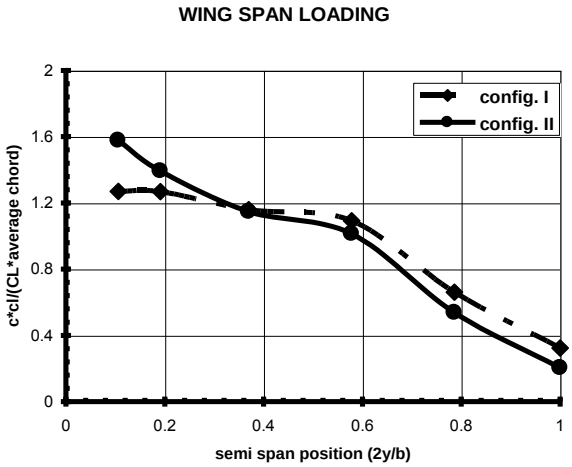

Fig. 12 Wing span loading for configuration I and II

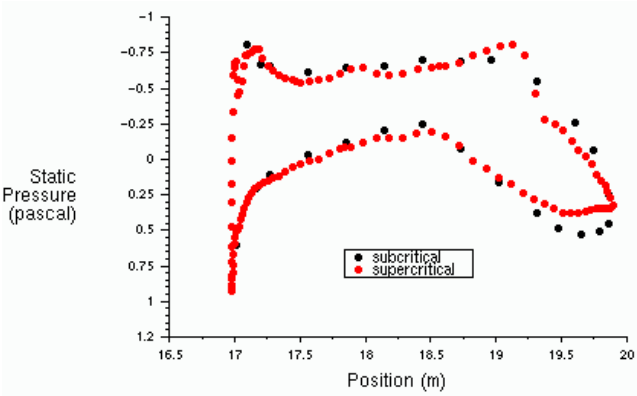

Fig. 13 The comparisons between pressure distribution at subcritical Mach number and design Mach number for outboard wing section (at C_L = 0.5)

4 Discussion

The two-dimensional verification check showed that the pressure distribution predicted by RAMPANT was in fair agreement with the calculated data from Boeing/NASA (Figure 3). The shock position and strength were quite close. The RAMPANT method predicted that the NLF-5 airfoil had more lift aft of the shock and less lift in the front of shock, hence more pitching moment.

The three-dimensional RAMPANT pressure distribution prediction at spanwise station 0.46 was in fair agreement with the calculated data by TIBLT code (Figure 4). A shock is present on the upper surface of the wing. The shock position predicted by RAMPANT was about 5 % of the chord length aft of the TIBLT prediction. This may be because the grid was not fine enough (because the limitations of available computer memory) to capture the shock.

The W-ATRA wing configuration results were produced from only the first iteration of a very complex wing design process. The above wing is not yet optimum both for undeflected and deflected VC flap. Due to the limitations of time and computer memory, the first author can not analyze the VC at several flight conditions (at design point as well as off-design) to show its biggest benefit. Regardless of its weakness, its performance appears quite reasonable, and almost met the aerodynamic design objectives as described on section 3.1.

To improve the wing aerodynamic performance, it is recommended that further optimization be made of the airfoil sections, twist and VC-flap deflection distributions along the wing span, together with laminar suction requirements.

5 Conclusion

A methodology has been developed for the aerodynamic wing design using CFD, allowing for the use of combined laminar and variable camber flap/wing concepts for transonic transport aircraft.

To simulate the real flow, the grid should be fine enough, especially in the region of high curvature (e.g. leading edge), the grid adjacent to the wall and in the regions of high pressure gradients.

The CFD simulations can save the design costs during the development of the new transport aircraft project by reducing the need for some wind tunnel testing and flight tests.

The conclusion can finally be drawn, that Computational Fluid Dynamic (CFD) is technically and economically feasible as a powerful design tool to optimize the aerodynamic wing shape.

References:

[1] H K Versteeg and W Malalasekera, *An Introduction To Computational Fluid Dynamics, The Finite Volume Method*, Longman Group Ltd., 1995.

[2] W.H. Li and X.Z. Zhang, "Simulation Study of Particle Motion in a Micro-Fluidic Dielectrophoretic Device," *WSEAS TRANSACTIONS on Fluid Mechanics*, Issue 8, Volume 1, August 2006, ISSN 1790-5087, page 850-855.

[3] W.H. Li, J. Sun and X.Z. Zhang, "Quadrupole Dielectrophoretic Device for Particle Trapping : A Numerical Study," *WSEAS TRANSACTIONS on Fluid Mechanics*, Issue 8, Volume 1, August 2006, ISSN 1790-5087, page 825-831.

[4] Prasetyo Edi, "An Aircraft Family Concept for a High Subsonic Regional Aircraft," *WSEAS/IASME TRANSACTIONS Journal on Fluid Mechanics and Aerodynamics*, Issue 7, Volume 2, September 2005, ISSN 1790-031X, page 1140-1148.

[5] Bento Silva de Mattos (EMBRAER, Brazil), Computer Simulations Save US$ 150,000 in Commuter Jet Design by Reducing Wind Tunnel Testing, *Journal Articles by Fluent Software Users*, JA096, 1999, pp. 1-4.

[6] Edi, P., *"Investigation of the application of hybrid laminar flow control and variable camber wing design for regional aircraft,"* PhD thesis, AVT/CoA/Cranfield University, Cranfield – UK, 1998.

[7] Boeing Commercial Airplane Company, *"Natural Laminar Flow Airfoil Analysis and Trade Studies Final Report,"* NASA CR 159029, August 1977 - June 1979.

[8] Shawn H. Woodson and R. DeJarnette, *"A Transonic Interactive Boundary-Layer Theory for Laminar and Turbulent Flow Over Swept Wings,"* NASA CR 4185, 1988.

[9] Hussein, A. S., "Comparative Study between Inviscid and Viscous Computations of Transonic Limit Cycle Oscillations for a Sweptback Supercritical Airfoil," *The International Journal of Intelligent Computing and Information Sciences (IJICIS)*, Vol. 4, No. 1, January 2004.

[10] Baker, M. D., Mathias, D. L., Roth, K. R., and Cummings, R.M., "Numerical Investigation of Slat and Compressibility Effects for a High-Lift Wing," *Journal of Aircraft*, Vol. 39, No. 5, September-October 2002.